

# Quantifying the Electrocatalytic Turnover of Vitamin B<sub>12</sub>-Mediated Dehalogenation on Single Soft Nanoparticles

Wei Cheng and Richard G. Compton\*

**Abstract:** We report the electrocatalytic dehalogenation of trichloroethylene (TCE) by single soft nanoparticles in the form of Vitamin B<sub>12</sub>-containing droplets. We quantify the turnover number of the catalytic reaction at the single soft nanoparticle level. The kinetic data shows that the binding of TCE with the electro-reduced vitamin in the Co<sup>I</sup> oxidation state is chemically reversible.

Measuring the catalytic kinetics of individual nanoparticles is challenging because the charge transfer can only be crudely estimated when using an ensemble. As a result, single nanoparticles measurements are essential.<sup>[1]</sup> An electrochemical method using the so-called nano-impacts has been recently developed to characterize individual nanoparticles when they randomly collide, by virtue of their Brownian motion, with a potentiostated electrode.<sup>[2]</sup> Electrocatalytic reactions at the surface of single metal nanoparticles can be observed when such nanoparticles impact an inert electrode that otherwise could not electrocatalyze. Most recently, the nano-impacts approach has been extended to characterize single soft nanoparticles,<sup>[3]</sup> such as liposomes,<sup>[3a]</sup> vesicles,<sup>[3b]</sup> viruses,<sup>[3c]</sup> micelles,<sup>[3d]</sup> droplets and mediated oxygen reduction,<sup>[3e–j]</sup> and macromolecules.<sup>[3k–n]</sup> Electron transfer is revealed by probing redox molecules or catalysts encapsulated inside soft nanoparticles, in contrast to the mediated charge transfer that takes place at the surface of metal nanoparticles. To date, there are few reports on reactions catalyzed by soft nanoparticles compared to the extensive studies on metal nanocatalysts.<sup>[4]</sup> In particular, the kinetics and single turn-over efficiency of soft nanoparticles of any type have never been quantified with single-nanoparticle resolution.

As a natural redox enzyme, electron transfer through Co<sup>III</sup>, the redox center in Vitamin B<sub>12</sub> (VB<sub>12</sub>), has found diverse uses in synthesis, bioremediation, and biocatalysis.<sup>[5]</sup> There has been significant interest in electrocatalytic reactions by Vitamin B<sub>12</sub>.<sup>[6]</sup> In particular, the reductive dehalogenation through Co<sup>III</sup> has attracted large interest<sup>[6a,d]</sup> and recently was suggested to occur via the intermediary of halogen-cobalt bond formation.<sup>[7]</sup> Using Vitamin B<sub>12</sub> as a model system, we report the electrocatalytic dehalogenation

of trichloroethylene (TCE) by single soft nanoparticles (nano-droplet) that contain Vitamin B<sub>12</sub> dissolved in water/glycerol encapsulated by emulsifiers. We find that the binding between Co<sup>I</sup>, the reduced form of Co<sup>III</sup>, and TCE is likely a chemically reversible process, and quantify the catalytic efficiency, interrogating soft nanoparticle catalysis at the single-nanoparticle level in real time with single-turnover resolution. To our knowledge, this is the first report to semi-quantitatively measure the turnover number and the kinetics of catalytic reactions at individual soft nanoparticles.

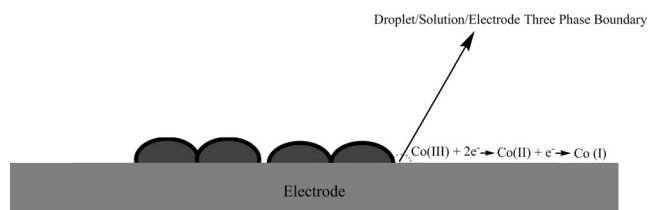
The ensemble electrochemical behavior of VB<sub>12</sub> emulsions was first investigated by dropcasting emulsions of droplets to form an ensemble on a macro glassy carbon (GC) electrode (diameter=3 mm) and recording cyclic voltammograms. Figure S1a in the Supporting Information shows the cyclic voltammograms for a glassy carbon macro-electrode modified with 2  $\mu$ L VB<sub>12</sub> droplets immersed in phosphate buffered saline (PBS) buffer (pH 6.9) at different scans between 20 mV s<sup>-1</sup> to 400 mV s<sup>-1</sup>. Two reduction peaks were observed around -0.10 V and -0.95 V versus the saturated calomel reference electrode (SCE), likely corresponding to the two stages of one-electron transfer: Co<sup>III</sup> + e<sup>-</sup> → Co<sup>II</sup> (Eq. 1) and Co<sup>II</sup> + e<sup>-</sup> → Co<sup>I</sup> (Eq. 2), respectively.<sup>[8]</sup>

The peak current shows a linear dependence on scan rates (Figure S1b), indicating a surface-controlled process, while the integrated charge under the first reductive peak amounts to less than 2% of the total theoretical charge, assuming the immobilized VB<sub>12</sub> droplets are completely reduced from Co<sup>III</sup> to Co<sup>II</sup> and knowing the mass of material dropcasted (Supporting Information). It was inferred that the charge injection occurred at the three-phase boundary formed between the surface-immobilized droplets, the electrode, and the solution<sup>[9]</sup> (Scheme 1).

Voltammetric methods were further used to study the electrocatalytic behavior of immobilized VB<sub>12</sub> droplets in the presence of TCE, as shown in Figure 1. It was found that addition of TCE caused a large increase in the second electron transfer between Co<sup>II</sup> and Co<sup>I</sup> at -1.1 V, which is attributed to the catalytic reduction of TCE. Comparing the

[\*] Dr. W. Cheng, Prof. Dr. R. G. Compton  
Department of Chemistry  
Physical & Theoretical Chemistry Laboratory  
Oxford University  
South Parks Road, Oxford, OX1 3QZ (UK)  
E-mail: richard.compton@chem.ox.ac.uk

Supporting information for this article is available on the WWW under <http://dx.doi.org/10.1002/anie.201510394>.



**Scheme 1.** Reduction of Vitamin B<sub>12</sub> droplets dropcast on a macro electrode.

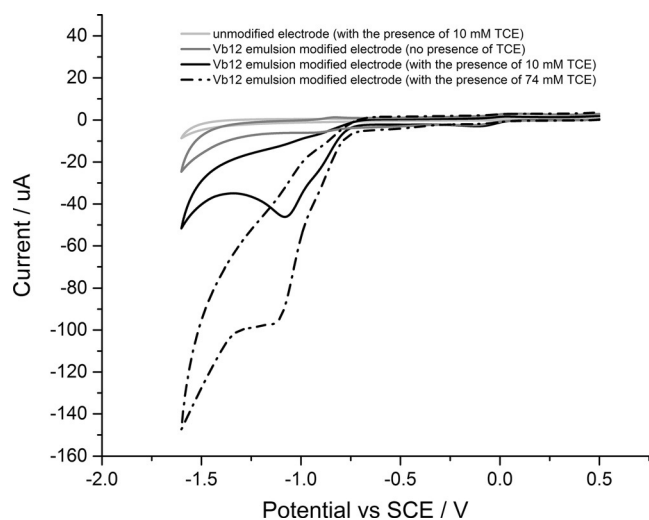


**Figure 1.** Ensemble voltammograms of glassy carbon electrode modified with VB<sub>12</sub> droplets at 200 mVs<sup>-1</sup> in 100 mM PBS buffer (pH 6.9) containing 74 mM TCE (black dash dot), 10 mM TCE (black line), 0 mM TCE (gray line) and voltammogram of bare glassy carbon electrode in PBS buffer containing 10 mM TCE (pH 6.9) (light gray line).

voltammograms without TCE (gray line) or without VB<sub>12</sub> (light gray line) clearly demonstrates the electrocatalytic activity of VB<sub>12</sub> droplets modified on the electrode for the reduction of trichloroethylene  $\text{Co}^{\text{III}} + 2\text{e}^- \rightarrow \text{Co}^{\text{I}}$ , followed by the reduction of TCE through  $\text{Co}^{\text{I}}$ , with dichloroethylene (DCE) as a product.<sup>[6d,f]</sup>



Whilst the voltammetry indicates catalysis of the reduction of TCE by the  $\text{Co}^{\text{III}}$  oxidative state of VB<sub>12</sub> (Figures 1, S1 and S2), because of the uncertain geometry of the droplet-modified electrode and the imprecise nature of the three-phase boundary, it is hard, if not impossible, to extract quantitative information. We therefore turned to nano-impacts to clarify and quantify the kinetics and mechanism. The three-phase boundary restriction is not likely to apply to single nanodroplets because complete electrolysis has been shown for VB<sub>12</sub> droplets,<sup>[3e]</sup> and similar data has also been reported by others on soft nanoparticles.<sup>[3f,g]</sup> The differences may arise because of possible coalescence of nanodroplets on the electrode surface.

Next, a carbon microelectrode was immersed in PBS buffer solution and known amounts of dispersed VB<sub>12</sub> droplets and trichloroethylene added. In the absence of TCE, clear reductive (Faradaic) current spikes were detected at potentials more negative than -0.3 V (Figure 2a). A plot of average charge resulting from the reduction of individual VB<sub>12</sub> nanodroplets versus applied potentials (voltammogram) was obtained by recording the average charge (the number of recorded impact events for each potential was greater than 100) transferred as a result of direct Faradaic reduction of VB<sub>12</sub> droplets at different potentials (Figure 2b). The onset of the spikes were found to be dependent on the reduction potential, and no reductive spikes of VB<sub>12</sub> droplets were seen

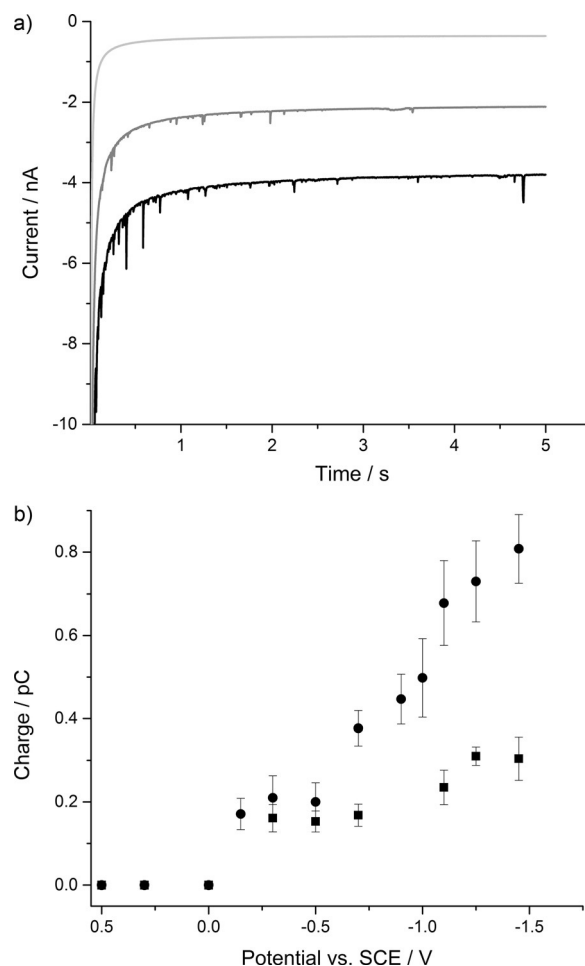


**Figure 2.** a) Representative chronoamperometric profiles of nano-impacts at -1.25 V versus SCE, in PBS buffer (100 mM; pH 6.9) containing: 16 mM TCE only (light gray line); VB<sub>12</sub> nanodroplets only (gray line); VB<sub>12</sub> nanodroplets and 16 mM TCE (black line); b) voltammograms of single soft nanoparticles: VB<sub>12</sub> nanodroplets only (black squares), VB<sub>12</sub> nanodroplets and 16 mM TCE (black dots).

at the reductive potentials of +0.1 V or more positive, suggesting the spikes correspond to Faradaic reduction of VB<sub>12</sub>-containing droplets. The presence of two plateaus in this voltammogram suggest two steps of reduction of single droplets containing VB<sub>12</sub>, respectively resulting from the reduction of  $\text{Co}^{\text{III}}$  to  $\text{Co}^{\text{II}}$ , and the subsequent reduction of  $\text{Co}^{\text{II}}$  to  $\text{Co}^{\text{I}}$  upon a single droplet impacting at higher potential. The average charge value at second plateau is almost twice of that at the first plateau, consistent with double-electron transfer occurring during single nanoparticle impacts at very negative potentials.

Analogous nano-impact experiments of single VB<sub>12</sub> droplets were conducted in PBS buffer containing 16 mM TCE. At lower potential (up to -0.5 V), the amplitudes of spikes are similar to those found without TCE, while the amplitude of the spikes significantly increased when the potential was -0.75 V or more negative (Figure 2), indicating that at a sufficiently high potential, TCE is involved in charge transfer and is reduced when single VB<sub>12</sub> droplets collide with the electrode.

To further investigate the catalytic reduction of TCE by single VB<sub>12</sub> droplets, the average charge of individual spikes at a range of potentials was calculated and plotted as a function of potential (Figure 2b). Comparing this catalytic voltammogram of single VB<sub>12</sub> droplets (circles) to the voltammogram of direct reduction of single VB<sub>12</sub> droplets (squares), the average charge of individual spikes was found to be significantly larger at potentials above  $-0.75$  V, suggesting that catalytic reduction of TCE accompanies the direct reduction of single nanodroplets and contributes to the charge injection when individual VB<sub>12</sub> nanodroplets collide with the electrode. In contrast, the average charge of individual spikes is similar at potentials below  $-0.5$  V, indicating that the catalytic reduction of TCE can only accompany the electron transfer between Co<sup>II</sup> to Co<sup>I</sup> under a high potential, and the active catalyst is the reduced form Co<sup>I</sup>.<sup>[6a,d]</sup>

To obtain kinetic information on the reduction of TCE catalyzed by the single soft nanoparticles of VB<sub>12</sub>-containing droplets, catalytic voltammograms were obtained under different added concentrations of TCE (Figure 3). The amplitudes of spikes at certain high potentials generally increased with increasing concentrations of TCE, further confirming that the spikes observed at higher potentials correspond to catalytic reduction of TCE through single VB<sub>12</sub> nanodroplets impacting the electrode. The distribution of the charge from electrocatalytic reduction by individual soft nanoparticles indicates the size distribution of single soft nanoparticles (Figure S4).

To estimate the catalytic efficiency of dehalogenation by single nanodroplets, we define the effective turn-over number ( $k_{\text{eff}}$ ) at different concentrations of TCE substrates for electrocatalytic dehalogenation at single VB<sub>12</sub> soft nanoparticle by Equation (4):

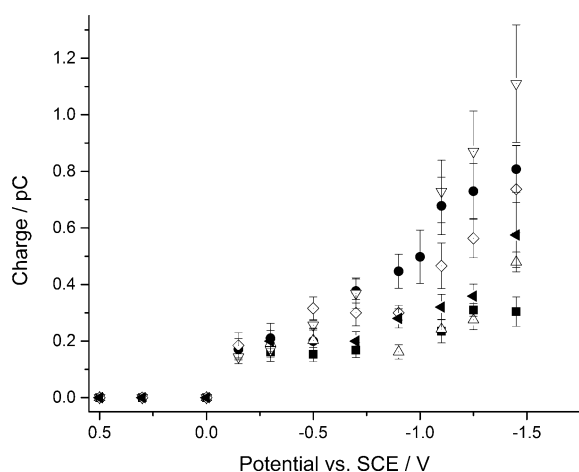
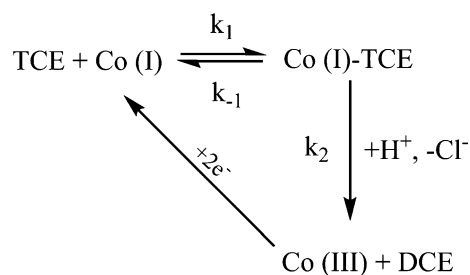


**Figure 3.** Catalytic voltammograms of single soft nanoparticles at various substrate concentrations: Average charge  $Q$  for single VB<sub>12</sub> droplets impacts vs. potential  $E$  in PBS buffer with increasing TCE concentrations: 0 mM (squares), 5 mM (up triangles), 7.4 mM (left triangles), 9.5 mM (diamonds), 16 mM (circles), and 74 mM (down triangles). The error of the mean charge is the standard error of the mean given by  $SD/\sqrt{n}$  where  $SD$  is the standard deviation and  $n$  is the sample number, in this case the number of spikes.<sup>[2]</sup>

$$k_{\text{eff}} = \frac{m}{tm_{\text{cat}}} = \frac{(Q_{\text{total}} - Q_1)}{tQ_1} \quad (4)$$

where  $m$  is the moles of TCE catalytically reduced or DCE catalytically produced,  $m_{\text{cat}}$  is the moles of catalyst, which in this case are the moles of VB<sub>12</sub> in single nano-droplets. Note that the charge transfer of single droplet is probably not limited by the surface area or the length of the three-phase boundary.<sup>[3]</sup> The charge transfer of a single nanodroplet  $Q_1$  is known to be quantitative and corresponds to the total amount of Vitamin B<sub>12</sub> catalysts encapsulated in single droplets.<sup>[3e]</sup>  $m_{\text{cat}}$  can be estimated as  $\frac{AQ_1}{2F}$ , where  $F$  is the Faraday constant,  $A$  is the Avogadro constant,  $Q_1$  is mean charge transferred for the reduction of single VB<sub>12</sub> nanodroplets without the presence of TCE corresponding to reduction of Co<sup>III</sup> to Co<sup>I</sup>.  $t$  is the duration of the impact times.  $m$  can be thus derived from the total mean charge ( $Q_{\text{total}}$ ) transferred for dehalogenation of trichloroethylene by single VB<sub>12</sub> nanodroplets (Figure 3), and the charge transferred ( $Q_1$ ) between Co<sup>III</sup> to Co<sup>I</sup> before the dehalogenation is initiated, as  $\frac{A(Q_{\text{total}} - Q_1)}{2F}$ . Two moles of electrons are transferred for catalytic dehalogenation from one mole TCE to DCE (Scheme 2).<sup>[6]</sup>



**Scheme 2.** Electrocatalytic reductive dehalogenation of TCE by VB<sub>12</sub>.

$k_{\text{eff}}$  can be estimated by Equation (4), using the mean charge (Figure 3) and impact times  $t$  obtained from nano-impacts experiments (Supporting Information) to be  $30 \pm 5$ ,  $44 \pm 9$ ,  $74 \pm 16$ ,  $81 \pm 8$ , and  $143 \pm 27$  s<sup>-1</sup> for various concentrations of TCE substrates from 5 mM up to 74 mM.<sup>[10]</sup> Furthermore, the effective turn-over number ( $k_{\text{eff}}$ ) at different concentrations of TCE substrates was plotted against the TCE concentration. Interestingly, a Michaelis–Menten-like response was observed (Figure S6), indicating a probably reversible binding between Co<sup>I</sup> and TCE (Scheme 2). If this is the case, when the concentration of TCE is sufficiently high so that all the reduced Co<sup>I</sup> forms of VB<sub>12</sub> in a single nanodroplet are actively bound, increasing TCE substrate will not increase the rate of the reaction beyond the maximum turn-over number the  $k_{\text{cat}}$ .

To verify the hypothesis and estimate the catalytic kinetics, the reaction rate of electrocatalytic dehalogenation is expressed as (Supporting Information):

$$\frac{d[\text{DCE}]}{dt} = \frac{k_2[\text{TCE}][\text{Co}^{\text{I}}]_{\text{total}}}{K + [\text{TCE}]} \quad (5)$$

thus

$$k_{\text{eff}} = \frac{k_{\text{cat}}[\text{TCE}]}{K + [\text{TCE}]} \quad (6)$$

then

$$\frac{1}{k_{\text{eff}}} = \frac{1}{k_{\text{cat}}} + \frac{K}{k_{\text{cat}}} \frac{1}{[\text{TCE}]} \quad (7)$$

where  $K$  is the kinetic constant  $\frac{(k_{-1}+k_2)}{k_1}$  (Supporting Information),  $[\text{TCE}]$  is the trichloroethylene concentration;  $[\text{DCE}]$  is the dichloroethylene concentration and  $[\text{Co}^{\text{I}}]_{\text{total}}$  is the total  $\text{Co}^{\text{I}}$  concentration.

The linear relation between  $\frac{1}{k_{\text{eff}}}$  and  $\frac{1}{[\text{TCE}]}$  is consistent with the proposed mechanism above for catalytic efficiency of dehalogenation by single soft nanoparticles. Furthermore, from the linear fitting by Equation (7) with the experimental data (Figure 4), the kinetic constant  $K$  and the maximum

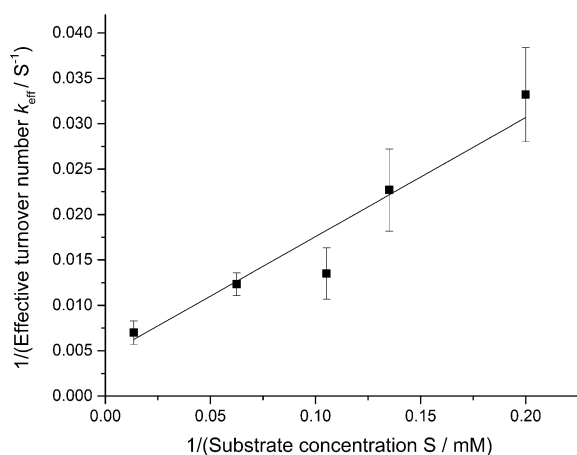


**Figure 4.** Catalytic kinetics of single soft nanoparticles: reciprocal of effective turnover number estimated according to Equation (1) versus reciprocal of TCE substrates (black squares), linear fitting (black line) to the experimental data given by Equation (7).

turnover number  $k_{\text{cat}}$  for single soft nanoparticles can be estimated as  $29 \pm 4 \text{ mM}$  and  $225 \pm 32 \text{ s}^{-1}$ , respectively. Then, the catalytic efficiency of single soft nanoparticles  $k_{\text{cat}}/K$  is estimated to be  $7.8 \times 10^3 \text{ M}^{-1} \text{ s}^{-1}$ , which is comparable to the value obtained from electrocatalytic reduction of ethylene dibromide in an emulsion system by Vitamin  $\text{B}_{12}$  molecules.<sup>[6g]</sup> The maximum turn-over number is found to be higher than the dehalogenation reported for Vitamin  $\text{B}_{12}$  molecules covalently immobilized onto the electrode, where in the latter case a multi-layer film was likely formed,<sup>[6c]</sup> while a complete electrolysis of Vitamin  $\text{B}_{12}$  molecules encapsulated within single nanodroplets is thought to occur.

To our knowledge, this is the first time that the kinetics and turnover frequency of single individual soft nanoparticles have been semi-quantitatively measured and analyzed. We believe this is a new strategy to fundamentally explore catalytic reactions of soft nanoparticles with the mechanistic simplification allowing insights into catalytic kinetics at

single-nanoparticle resolution, likely opening doors for discoveries and rational designs of soft nanoparticles and enzyme nanocarriers that are currently neglected but hold promise as more affordable and natural non-metal catalysts for diverse chemical reactions and applications.

## Acknowledgements

The European Research Council under the European Union's Seventh Framework Programme (ERC Grant Agreement n. [320403]) is gratefully acknowledged for funding this work. We thank Dr. D. Omanović (Center for Marine and Environmental Research Zagreb, Croatia) for developing Signal Counter software for data analysis.

**Keywords:** catalysis · electrochemistry · kinetics · soft nanoparticles · turnover numbers

**How to cite:** *Angew. Chem. Int. Ed.* **2016**, 55, 2545–2549

*Angew. Chem.* **2016**, 128, 2591–2595

- [1] a) P. Chen, X. C. Zhou, N. M. Andoy, K. S. Han, E. Choudhary, N. M. Zou, G. Q. Chen, H. Shen, *Chem. Soc. Rev.* **2014**, 43, 1107–1117; b) X. N. Shan, I. Diez-Perez, L. J. Wang, P. Wiktor, Y. Gu, L. H. Zhang, W. Wang, J. Lu, S. P. Wang, Q. H. Gong, J. H. Li, N. J. Tao, *Nat. Nanotechnol.* **2012**, 7, 668–672; c) W. L. Xu, J. S. Kong, Y. T. E. Yeh, P. Chen, *Nat. Mater.* **2008**, 7, 992–996; d) Y. W. Zhang, J. M. Lucas, P. Song, B. Beberwyck, Q. Fu, W. L. Xu, A. P. Alivisatos, *Proc. Natl. Acad. Sci. USA* **2015**, 112, 8959–8964.
- [2] a) S. E. Fosdick, M. J. Anderson, E. G. Nettleton, R. M. Crooks, *J. Am. Chem. Soc.* **2013**, 135, 5994–5997; b) R. Dasari, D. A. Robinson, K. J. Stevenson, *J. Am. Chem. Soc.* **2013**, 135, 570–573; c) A. J. Bard, H. J. Zhou, S. J. Kwon, *Isr. J. Chem.* **2010**, 50, 267–276; d) W. Cheng, R. G. Compton, *TrAC Trends Anal. Chem.* **2014**, 58, 79–89; e) N. V. Rees, *Electrochem. Commun.* **2014**, 43, 83–86; f) L. Wang, A. Ambrosi, M. Pumera, *Angew. Chem. Int. Ed.* **2013**, 52, 13818–13821; *Angew. Chem.* **2013**, 125, 14063–14066; g) M. Pumera, *ACS Nano* **2014**, 8, 7555–7558; h) J. M. Kahk, N. V. Rees, J. Pillay, R. Tshikhudo, S. Vilakazi, R. G. Compton, *Nano Today* **2012**, 7, 174–179; i) Y. G. Zhou, N. V. Rees, R. G. Compton, *Angew. Chem. Int. Ed.* **2011**, 50, 4219–4221; *Angew. Chem.* **2011**, 123, 4305–4307; j) E. J. E. Stuart, K. Tschulik, C. Batchelor-McAuley, R. G. Compton, *ACS Nano* **2014**, 8, 7648–7654; k) W. Cheng, X. F. Zhou, R. G. Compton, *Angew. Chem. Int. Ed.* **2013**, 52, 12980–12982; *Angew. Chem.* **2013**, 125, 13218–13220; l) X. Y. Xiao, A. J. Bard, *J. Am. Chem. Soc.* **2007**, 129, 9610–9612; m) X. Y. Xiao, F. R. F. Fan, J. P. Zhou, A. J. Bard, *J. Am. Chem. Soc.* **2008**, 130, 16669–16677.
- [3] a) W. Cheng, R. G. Compton, *Angew. Chem. Int. Ed.* **2014**, 53, 13928–13930; *Angew. Chem.* **2014**, 126, 14148–14150; b) J. Dunevall, H. Fathali, N. Najafinobar, J. Lovric, J. Wigstrom, A. S. Cans, A. G. Ewing, *J. Am. Chem. Soc.* **2015**, 137, 4344–4346; c) J. E. Dick, A. T. Hilterbrand, A. Boika, J. W. Upton, A. J. Bard, *Proc. Natl. Acad. Sci. USA* **2015**, 112, 5303–5308; d) H. S. Toh, R. G. Compton, *Chem. Sci.* **2015**, 6, 5053–5058; e) W. Cheng, R. G. Compton, *Angew. Chem. Int. Ed.* **2015**, 54, 7082–7085; *Angew. Chem.* **2015**, 127, 7188–7191; f) B. K. Kim, J. Kim, A. J. Bard, *J. Am. Chem. Soc.* **2015**, 137, 2343–2349; g) B. K. Kim, A. Boika, J. Kim, J. E. Dick, A. J. Bard, *J. Am. Chem. Soc.* **2014**, 136, 4849–4852; h) J. E. Dick, C. Renault, B. K. Kim, A. J. Bard, *Angew. Chem. Int. Ed.* **2014**, 53, 11859–11862; *Angew.*



- Chem.* **2014**, *126*, 12053–12056; i) J. E. Dick, C. Renault, B. K. Kim, A. J. Bard, *J. Am. Chem. Soc.* **2014**, *136*, 13546–13549; j) X. Li, S. Majdi, J. Dunevall, H. Fathali, A. G. Ewing, *Angew. Chem. Int. Ed.* **2015**, *54*, 11978–11982; *Angew. Chem.* **2015**, *127*, 12146–12150; k) X. F. Zhou, W. Cheng, R. G. Compton, *Angew. Chem. Int. Ed.* **2014**, *53*, 12587–12589; *Angew. Chem.* **2014**, *126*, 12795–12797; l) J. E. Dick, C. Renault, A. J. Bard, *J. Am. Chem. Soc.* **2015**, *137*, 8376–8379; m) X. F. Zhou, W. Cheng, R. G. Compton, *Nanoscale* **2014**, *6*, 6873–6878; n) X. F. Zhou, W. Cheng, R. G. Compton, *Nanoscale* **2015**, *7*, 15719–15726; o) C. E. Banks, N. V. Rees, R. G. Compton, *J. Electroanal. Chem.* **2002**, *535*, 41–47; p) C. E. Banks, N. V. Rees, R. G. Compton, *J. Phys. Chem. B* **2002**, *106*, 5810–5813.
- [4] a) S. Nayak, L. A. Lyon, *Angew. Chem. Int. Ed.* **2005**, *44*, 7686–7708; *Angew. Chem.* **2005**, *117*, 7862–7886; b) S. E. F. Kleijn, S. C. S. Lai, M. T. M. Koper, P. R. Unwin, *Angew. Chem. Int. Ed.* **2014**, *53*, 3558–3586; *Angew. Chem.* **2014**, *126*, 3630–3660; c) F. Zaera, *Chem. Soc. Rev.* **2013**, *42*, 2746–2762.
- [5] a) F. Zelder, *Chem. Commun.* **2015**, *51*, 14004–14017; b) M. Giedyk, K. Goliszewskaab, D. Gryko, *Chem. Soc. Rev.* **2015**, *44*, 3391–3404.
- [6] a) C. Costentin, M. Robert, J. M. Saveant, *J. Am. Chem. Soc.* **2005**, *127*, 12154–12155; b) S. T. Chang, C. H. Wang, H. Y. Du, H. C. Hsu, C. M. Kang, C. C. Chen, J. C. S. Wu, S. C. Yen, W. F. Huang, L. C. Chen, M. C. Lin, K. H. Chen, *Energy Environ. Sci.* **2012**, *5*, 5305–5314; c) H. Shimakoshi, M. Tokunaga, K. Kuroiwa, N. Kimizuka, Y. Hisaeda, *Chem. Commun.* **2004**, 50–51; d) T. F. Connors, J. V. Arena, J. F. Rusling, *J. Phys. Chem.* **1988**, *92*, 2810–2816; e) D. Lexa, J. M. Saveant, *Acc. Chem. Res.* **1983**, *16*, 235–243; f) Y. H. Kim, E. R. Carraway, *Environ. Technol.* **2002**, *23*, 1135–1145; g) J. F. Rusling, C. L. Miaw, E. C. Couture, *Inorg. Chem.* **1990**, *29*, 2025–2027; h) C. K. Njue, B. Nuthakki, A. Vaze, J. M. Bobbitt, J. F. Rusling, *Electrochem. Commun.* **2001**, *3*, 733–736.
- [7] K. A. P. Payne, C. P. Quezada, K. Fisher, M. S. Dunstan, F. A. Collins, H. Sjuts, C. Levy, S. Hay, S. E. J. Rigby, D. Leys, *Nature* **2015**, *517*, 513–516.
- [8] a) J. F. Rusling, T. F. Connors, A. Owlia, *Anal. Chem.* **1987**, *59*, 2123–2127; b) P. Tomčík, C. E. Banks, T. J. Davies, R. G. Compton, *Anal. Chem.* **2004**, *76*, 161–165.
- [9] a) F. Scholz, S. Komorsky-Lovric, M. Lovric, *Electrochem. Commun.* **2000**, *2*, 112–118; b) S. Komorsky-Lovrić, M. Lovrić, F. Scholz, *J. Electroanal. Chem.* **2001**, *508*, 129–137; c) M. Donten, Z. Stojek, F. Scholz, *Electrochem. Commun.* **2002**, *4*, 324–329; d) C. E. Banks, T. J. Davies, R. G. Evans, G. Hignett, A. J. Wain, N. S. Lawrence, J. D. Wadhawan, F. Marken, R. G. Compton, *Phys. Chem. Chem. Phys.* **2003**, *5*, 4053–4069; e) T. J. Davies, A. C. Garner, S. G. Davies, R. G. Compton, *J. Electroanal. Chem.* **2004**, *570*, 171–185.
- [10] E. Kätelhön, R. G. Compton, *Chem. Sci.* **2014**, *5*, 4592–4598.

Received: November 9, 2015

Revised: December 1, 2015

Published online: January 25, 2016